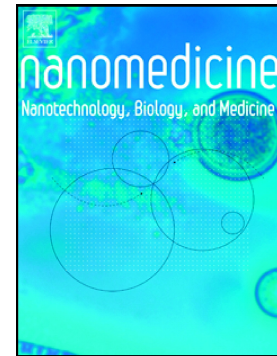


Raman spectroscopy reveals biochemical differences in plasma derived extracellular vesicles from sporadic amyotrophic lateral sclerosis patients

Carlo F. Morasso, Daisy Sproviero, Maria Chiara Mimmi, Marta Giannini, Stella Gagliardi, Renzo Vanna, Luca Diamanti, Stefano Bernuzzi, Francesca Piccotti, Marta Truffi, Orietta Pansarasa, Fabio Corsi, Cristina Cereda



PII: S1549-9634(20)30103-9

DOI: <https://doi.org/10.1016/j.nano.2020.102249>

Reference: NANO 102249

To appear in: *Nanomedicine: Nanotechnology, Biology, and Medicine*

Revised date: 4 June 2020

Please cite this article as: C.F. Morasso, D. Sproviero, M.C. Mimmi, et al., Raman spectroscopy reveals biochemical differences in plasma derived extracellular vesicles from sporadic amyotrophic lateral sclerosis patients, *Nanomedicine: Nanotechnology, Biology, and Medicine* (2020), <https://doi.org/10.1016/j.nano.2020.102249>

This is a PDF file of an article that has undergone enhancements after acceptance, such as the addition of a cover page and metadata, and formatting for readability, but it is not yet the definitive version of record. This version will undergo additional copyediting, typesetting and review before it is published in its final form, but we are providing this version to give early visibility of the article. Please note that, during the production process, errors may be discovered which could affect the content, and all legal disclaimers that apply to the journal pertain.

Raman Spectroscopy reveals biochemical differences in plasma derived extracellular vesicles from sporadic Amyotrophic Lateral Sclerosis patients.

Carlo F. Morasso, Dr.^{1,*,#}, Daisy Sproviero, Dr.^{2,#}, Maria Chiara Mimmi, Dr.², Marta Giannini, Dr.^{2,3}, Stella Gagliardi, Dr.², Renzo Vanna, Dr.¹, Luca Diamanti, Dr.⁴, Stefano Bernuzzi, Dr.⁵, Francesca Piccotti, M.Sc.¹, Marta Truffi, Dr.¹, Orietta Pansarasa, Dr.², Fabio Corsi, Prof.^{1,6}, Cristina Cereda, Dr.^{2,*}

- 1) Istituti Clinici Scientifici Maugeri IRCCS, Pavia, Italy
- 2) Genomic and post-Genomic Center, IRCCS Mondino Foundation, Pavia, Italy
- 3) Department of Brain and Behavioural Sciences, University of Pavia, Pavia, Italy
- 4) Unit of General Neurology, IRCCS Mondino Foundation, Pavia, Italy
- 5) Immunohematological and Transfusional Service and Centre of Transplantation Immunology, IRCCS “San Matteo Foundation”, Pavia, Italy
- 6) Department of Biomedical and Clinical Sciences “Luigi Sacco”, University of Milan, Milano, Italy.

Corresponding Authors:

* Carlo F. Morasso: e-mail: carlo.morasso@icsmaugeri.it
Laboratory of Nanomedicine and Molecular Imaging
Istituti Clinici Scientifici Maugeri IRCCS
Via Maugeri 4, 27100, Pavia – Italia
Phone: +39 0382 592209
Twitter: @MorassoCa

* Cristina Cereda: e-mail: cristina.cereda@mondino.it
Genomic and post-Genomic Center,
IRCCS Mondino Foundation,
Via Mondino, 2, 27100 Pavia, Italy.
Phone: +39 0382-380348/248

Word count for abstract: 146 words

Word count for manuscript: 4628 words

Number of references: 41

Number of figures: 6

Number of tables: 1

Number of Supplementary online-only files: 1

Journal Pre-proof

ABSTRACT: Sporadic Amyotrophic Lateral Sclerosis (ALS) is a neurodegenerative disease for which there is no validated blood based biomarker. Extracellular vesicles (EVs) have the potential to solve this unmet clinical need. However, due to their heterogeneity and complex chemical composition, EVs are difficult to study. Raman spectroscopy (RS) is an optical method that seems particularly well suited to address this task. In fact, RS provides an overview of the biochemical composition of EVs quickly and virtually without any sample preparation. In this work, we studied by RS small extracellular vesicles (sEVs), large extracellular vesicles (IEVs) and blood plasma of sporadic ALS patients and of a matched cohort of healthy controls. The obtained results highlighted IEVs as a particularly promising biomarker for ALS. In fact, their Raman spectra show that sporadic ALS patients have a different lipid content and less intense bands relative to the aromatic aminoacid phenylalanine.

HIGHLIGHTS':

- Raman detects differences between subtypes of extracellular vesicles (EVs)
- Large EVs have a different lipid and protein content in patients with ALS
- Large EVs are a promising biomarker for the diagnosis of ALS

KEYWORDS: Raman Spectroscopy; Amyotrophic Lateral Sclerosis; small extracellular vesicles (sEVs); large extracellular vesicles (IEVs); Plasma;

Journal Pre-proof

BACKGROUND:

Sporadic Amyotrophic Lateral Sclerosis (ALS) is a neurodegenerative disease that causes progressive muscle weakness through loss of upper and lower motor neurons (UMN and LMN) (1). No cure and biomarkers are currently available for this fatal disease and, in the last years, the search for new biomarkers have been the subject of ALS research (2). Circulating extracellular vesicles (EVs) have been suggested as possible biomarkers in neurological disorders (3). EVs are a heterogeneous family of membrane-based vesicles released by every cell and they are abundantly present in several biofluids such as plasma, urine and liquor (4) Previously, EVs used to be classified according to their size and biogenesis in microvesicles and exosomes. Microvesicles (MVs) were referred to vesicles with a dimension between 130 and 1000 nm that shed by outward blebbing of the plasma membrane of a cell. With the term exosomes (EXOs), instead, vesicles having dimension between 30 and 130 nm were defined, and they originate from the endosomes (5). According to the guidelines of the International Society for the study of Extracellular Vesicle (ISEV) released in 2018 MVs and EXOs couldn't be distinguished on a particular biogenesis pathway and so they were distinguished in small extracellular vesicles (sEVs) (30-130 nm) and large extracellular vesicles (IEVs) (130-1000 nm) mainly on their size (6).

We previously demonstrated significant differences between IEVs and sEVs in ALS. First of all, we demonstrated that IEVs derived from plasma of sporadic ALS patients (SALSs), but not sEVs, were enriched in toxic ALS-related proteins (SOD1, TDP-43 and FUS) respect to healthy controls (HCs) (7). We were thus interested in finding further possible biochemical variations between different types of EVs in ALS subjects and matched controls.

The study of EVs however is complex since, differently from the most studied proteins or DNAs, they have a complex biochemical composition made of lipids, proteins, RNAs/DNAs and small metabolites. Despite the technical challenge, the analysis of EVs extracted from peripheral blood

remain promising for biomarker discovery since the collection of EVS is minimally-invasive for patients and can provide biomarkers of great diagnostic and prognostic value (8).

Vibrational spectroscopies, and in particular Raman spectroscopy (RS) (9), are attractive tools for the study of EVs as they can provide in few minutes an overall biochemical characterization without using any particular reagent and without targeting any previously known marker (10). RS seems particularly well suited for the task since, being routinely coupled with a microscope, it can analyse very low amount of material, or even single EVs. Given this attractive characteristic, in the last years few groups applied RS for the characterization of EVs proving the effectiveness of this technique (11-14). Recently, RS was also demonstrated as able to identify a specific bio molecular pattern of EVs from patients affected by Parkinson's disease (15). In this work we thus decide to explore by RS the biochemical differences between IEVs, sEVs and blood plasma (PL). Once identified the differences among the EVs subpopulation and the plasma, the main aim of this work was the identification of the biomolecules present in IEVs and sEVs of SALSs and the comparison with a matched cohort of HCs. In this way, we were hoping to define a peculiar Raman profile that could be used as additional tool to help the diagnosis and/or prognosis of ALS.

METHODS:

Patient selection

ALS diagnosis was made according to the revised El Escorial Criteria (16) at Mondino Foundation (Pavia, Italy). Patients with concomitant comorbidity were excluded. Blood from 20 SALSs patients was collected (mean age: $65.9 \pm \text{sd } 10.9$). The Ethical Committee of Mondino Foundation IRCCS (Pavia, Italy) approved this study protocol for patients and controls. Subjects participating signed an informed consent (Protocol n. 375/04 – version 07/01/2004). See Table 1 for demographic and clinical characteristics. Progression rate at the last visit (PRL) was calculated as 48 minus the ALS

Functional Rating Scale–Revised score (ALSF_{RS}) at the last visit divided by the disease duration (in months) from onset of symptoms to the last visit ($(48-ALSF_{RS}/\Delta t)$) (17). Progression rate lower than 0.5, and higher than 1 distinguishes ALS-slow and ALS-fast. .

Sex- and age-matched HCs free from any pharmacological treatment were recruited at the Immunohematological and Transfusional Service and Centre of Transplantation Immunology IRCCS “San Matteo Foundation” (Pavia, Italy) after signature of the informed consent.

Journal Pre-proof

Variables	Data
Age	68 (SD 6.8 range 54-80)
Gender (Male/Female)	10/10
Site of onset (Spinal/bulbar)	14/6 (60/20)
ALSFRS (ALS Functional Rating Scale)	35.52 (SD 8.5; range:15-46)
PLR (Progression rate at the last visit)	Range 0.14-2.35
Fast/Slow (Fast-PRL>1; Slow-PRL<0.5)	10/10

Table 1. Characteristics of the sporadic ALS patients included in the study

Isolation of plasma and plasma derived IEVs and sEVs

Plasma, IEVs and sEVs were isolated as previously described (7, 18, 19). Briefly, venous blood (5 ml) was collected in sodium citrate tubes from SALSs and HCs. Within 1 h it was centrifuged at 1,000g for 15 min to separate plasma, followed by an additional centrifugation at 1,600g for 20 min to remove platelets. Plasma was then ready to be processed for RS. Platelet-free plasma was centrifuged at 20,000g for 1 h with Centrifuge 5427 R (Eppendorf, Italy). The obtained pellet contains IEVs. The pellet was washed with 0.22 μ m filtered PBS and centrifuged a second time 1 h at 20,000g. The resulting pellet was then processed for IEVs analysis. The supernatant of the previous centrifugation was filtered through a 0.2 μ m filter and spun in an Optima MAX-TL Ultracentrifuge at 100,000g for 1 h at 4°C. After ultracentrifugation, the supernatant was removed and the pellet containing sEVs was resuspended in 1 ml of filtered PBS and centrifuged again at 100,000g for 1 h at 4°C. The obtained sEVs pellet was processed for analysis. Figure S1 report a schematic description of the isolation protocol of IEVs and sEVs.

Nanoparticle-tracking analysis (NTA) of IEVs and sEVs

EVs from SALSs and HCs were analysed by nanoparticle-tracking analysis (NTA) using a NS300 instrument (NanoSight, Amesbury, UK) in order to detect size and concentration of IEVs and sEVs. For a more accurate detection, samples were diluted with filtered PBS to the optimal concentration (10^8 – 10^9 particles/ml). After dilution, 1 ml of diluted sample was loaded in the machine and read at a rate of about 30 frames/sec. Particle movement videos were recorded 3 times per test and dimension and EVs concentration were analysed by the NTA software (version 2.2, NanoSight). The results of NTA analysis were presented as the mean of the three tests.

Transmission electron microscopy (TEM)

Transmission electron microscopy was used to study the morphology of IEVs and sEVs. For TEM, 40 μ l of vesicle suspension were placed on a carbon-coated EM grid, and 0.4 μ l of 25% glutaraldehyde was added. Vesicles were then allowed to settle onto the grid overnight at 4°C. Grids were then blotted on filter paper and stained for 30 seconds with 2% uranyl acetate. After further blotting and drying, samples were directly observed on a Tecnai 10 TEM (FEI). Images were captured with a Megaview G2 camera and processed with iTEM and Adobe Photoshop software.

Protein extraction of IEVs and sEVs

IEVs and sEVs pellet were lysed in cold Radio-Immunoprecipitation Assay (RIPA) buffer containing a mixture of phosphatase and protease inhibitors (Sigma-Aldrich, Italy). They were incubated for 20 min in ice and centrifuged at 16,000g for 5 min at 4°C. The supernatant was transferred to a fresh tube and protein concentration was determined by BCA assay (Sigma-Aldrich, Italy). An amount of 30 μ g of IEVs and sEVs lysates was mixed with 2x SDS sample buffer and denatured at 95°C for 10 min.

Western blot analysis

Proteins were fractionated by size on SDS 12.5% polyacrylamide gels with a Mini-PROTEAN® Tetra Vertical Electrophoresis Cell (BioRad, Italy) transferred to a nitrocellulose membrane (BioRad, Italy), using a liquid transfer apparatus (Trans-blot, BioRad, Italy) and blocked with 5% non-fat dry milk in Tween-20 Tris-Buffered Saline solution (TBS-T) (blocking solution) for 1 h. Membranes were incubated overnight with an Anti-Annexin V (Santa Cruz Biotechnology, Inc., USA) or Anti-Alix (Abcam, Inc., USA) antibodies in blocking solution. Membranes were then incubated for 1 h at room temperature with donkey anti-mouse or rabbit secondary peroxidase-conjugated antibody (GE Healthcare, UK). Bands were visualized using an enhanced chemiluminescence detection kit (ECL Advance, Ge Healthcare, UK). For subsequent immunoreactions, primary and secondary antibodies were removed from the membrane with stripping solution (100 mM Glycine, 0,1% NP-40, 1% SDS pH 2.2) incubated for 20 min. Membranes were then washed with TBST and processed, as previously described.

Acquisition of Raman spectra, data processing and analysis

Raman spectra were acquired using an InVia Reflex confocal Raman microscope (Renishaw plc, Wotton-under-Edge, UK) equipped with a He-Ne laser light source operating at 633 nm. The Raman spectrometer was calibrated daily using the band at 520.7 cm^{-1} of a silicon wafer.

Typically, a $3.5\text{ }\mu\text{L}$ drop of sample was dropped on the surface of Raman-compatible CaF_2 discs (Crystran, UK) and dried for 20 minutes at room temperature. The Raman study was performed using a 633 nm excitation laser with 100% power (around 22 mW at source), a 1200 l/mm grating and a 100x objective.

Spectra were acquired in the region between 400 and 1800 cm^{-1} as sum of seven acquisitions of 10 seconds. Spectra resolution is about 1.7 cm^{-1} . For each sample, five different spectra were collected on different positions of the drop. The software package WIRE 5 (Renishaw, UK) was used for the

spectral acquisition and to remove cosmic rays. Background fluorescence was removed by an asymmetric least square smoothing method (20). The spectra acquired for each sample were vector normalized for comparison in the statistical analysis. Spectrum normalization and data analysis were performed using OriginPro, Version 2019 (OriginLab Corporation, Northampton, MA, USA). Continuous quantitative variables were analysed by Student's t-test after having confirmed that data are normally distributed by means of Kolmogorov-Smirnov normality test. The multivariate analysis of data was done using the Principal Component Analysis for spectroscopy tool function of OriginPro, Version 2019. Receiver Operating Characteristic were calculated using OriginPro, Version 2019 (OriginLab Corporation, Northampton, MA, USA).

RESULTS:

Characterization of Extracellular Vesicles

IEVs and sEVs were extracted from blood plasma of SALSs and HCs by differential centrifugation and filtration protocol (18) as previously described (7, 18, 19). Differential centrifugation consists of successive centrifugation steps with increasing centrifugation forces and durations, generally aimed at isolating smaller from larger objects. Larger particles are removed in the first centrifugation steps, sediment faster and leave most of the smaller particles in the supernatant. NTA was used to confirm their different dimension in size as reported in Figure 1A. TEM analysis also confirmed the difference in size of the two populations (Figure 1B). In order to confirm the correct purification of IEVs and sEVs, in accordance with the literature (5, 6) Annexin V (marker of IEVs) and Alix (marker of sEVs) were tested by WB analysis in all samples between SALSs and HCs subjects (Figure 1C). All the samples that had the right parameters in size and markers were analysed by Raman spectroscopy.

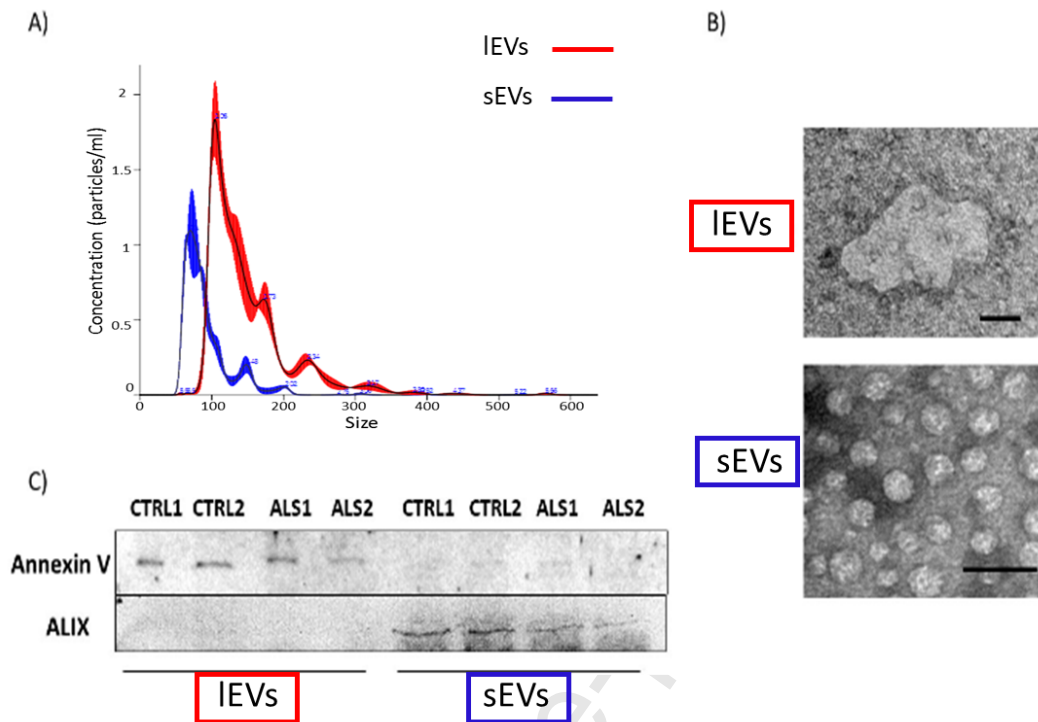


Figure 1: A) Nanosight profile of IEVs and sEVs from plasma. B) Representative images obtained by transmission electron microscopy (TEM) of IEVs and sEVs from plasma (Scale bar: 100 nm). C) Western Blot of IEVs and sEVs markers in IEVs and sEVs samples showed the presence of Annexin V only in IEVs pellet and Alix in sEVs fraction.

Raman analysis of plasma, IEVs and sEVs in healthy controls

Plasma derived IEVs and sEVs and PL sample from 20 HCs were analysed by RS using exactly the same procedure. From each sample, we collected five spectra. The average of five spectra was considered as representative for each sample and was considered independently in this analysis (total dataset 60 spectra). Spectra were acquired on the centre of the coffee ring formed upon drying of a drop of EVs and PL as shown in Figure S2 of the supporting information. This part of the

coffee ring showed the most intense spectra in the whole ring analysed and if free from the presence of signal coming from residual pf PBS as shown in Figure S3.

Figure 2 shows the average spectrum obtained from each preparation and the difference spectrum between them. While the general pattern remained constant, significant differences emerged in the intensity of the peaks present in the spectra. A table with the full assignment of the Raman bands observed, based on the scientific literature, is included in the supplementary information in Table S1. Peaks assignment was based on ref. 21-29.

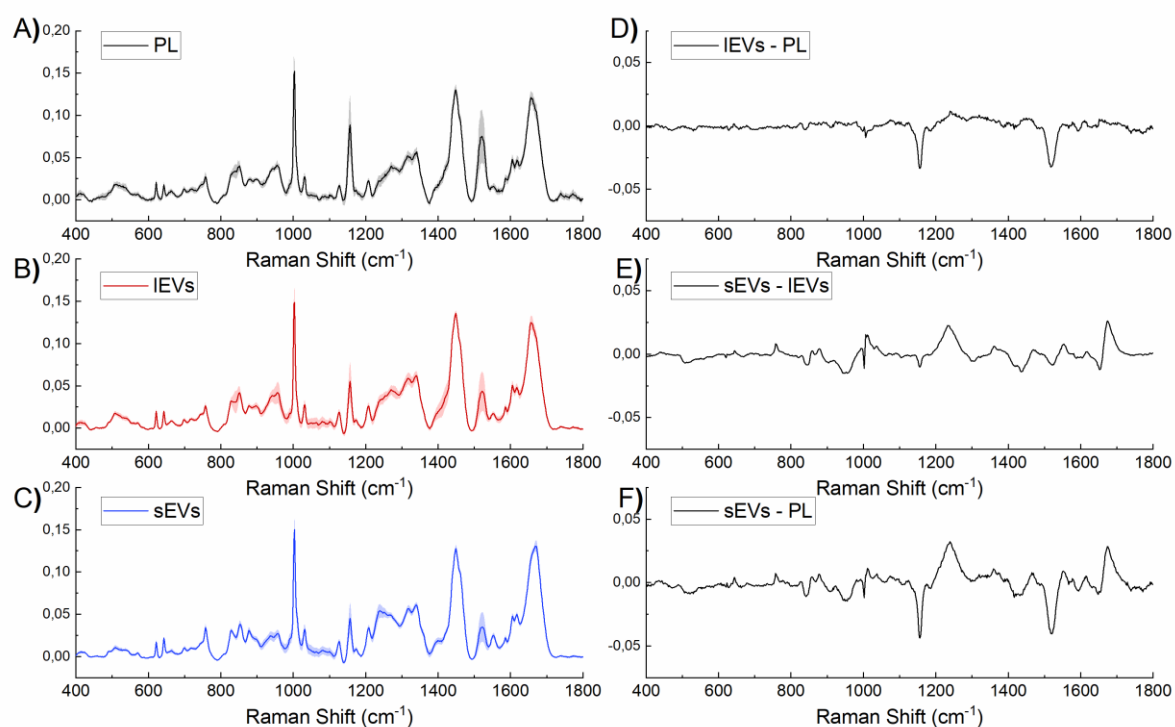


Figure 2. A) Average Raman spectrum of PL. B) Average Raman spectrum of IEVs. C) Average Raman spectrum of sEVs. D) Differential spectrum between IEVs and PL. E) Differential spectrum between IEVs and sEVs. F) Differential spectrum between sEVs and PL. The main line is the average of all samples. Shaded areas represent the standard deviation of the intensity.

Spectra highlighted the main differences between the three subgroups. In particular, Raman Spectra made clear that less intense peaks relative to carotenoids (at 1156 and 1519 cm^{-1}) characterized EVs when compared to PL. The bands relative to carotenoids showed a trend and were less intense in sEVs compared to PL and IEVs. Besides, we observed a progressive increase of the peaks relative to beta folded proteins (at 1239 and 1675 cm^{-1}) moving from PL to IEVs and sEVs.

A more detailed analysis of the intensity of selected peaks showed in Figure 3, proves that sEVs drastically differs from IEVs. In particular, the peak of tryptophan at 760 cm^{-1} was more intense in sEVs but did not vary between PL and IEVs. Similarly, the band relative to CH_2 of lipids at 1434 cm^{-1} was very similar in PL and IEVs but was much less intense in sEVs. sEVs also seemed to be characterized by peak relative to Amide III and Amide I with a higher content in β folded proteins than IEVs as proved by the more intense peak at 1239 cm^{-1} .

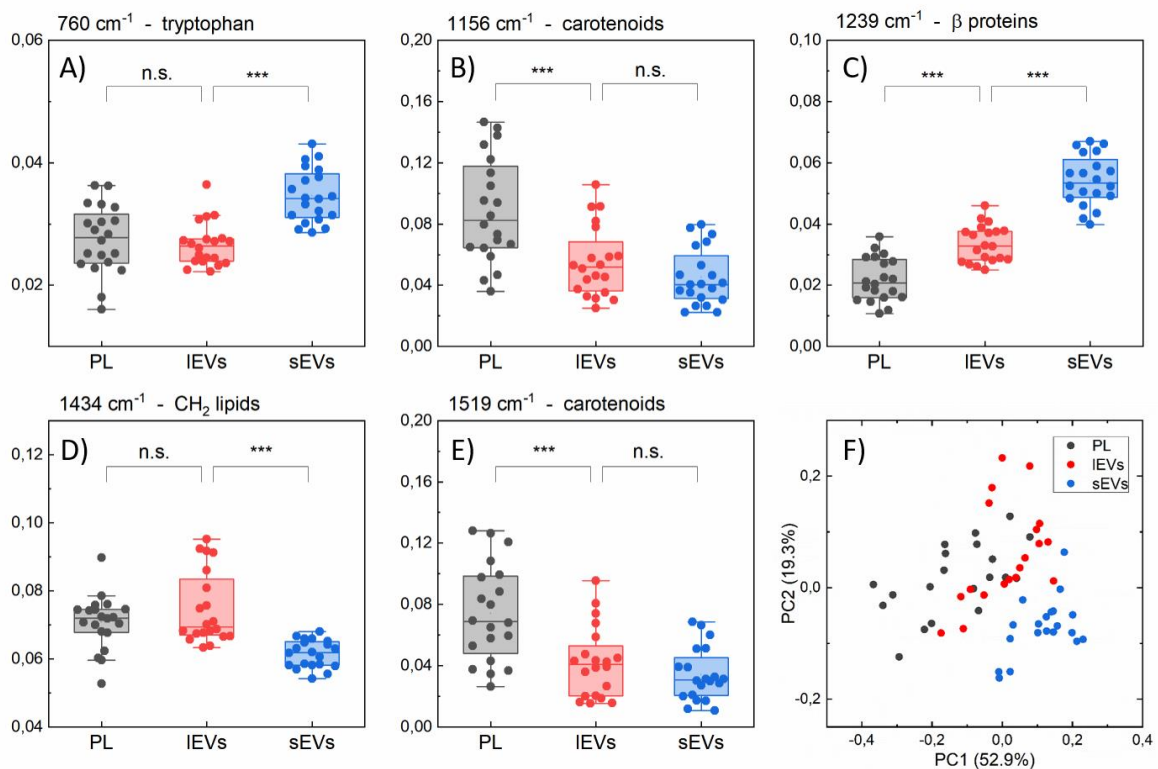


Figure 3: A-E) Box plot showing the different intensity of selected peaks of in the spectra of PL (grey), IEVs (red) and sEVs (blue). Data are shown as box and whiskers plots. Each data point represents a single subject acquired. Each box represents the 25th to 75th percentiles (interquartile range [IQR]). Lines inside the boxes represent the median. The whiskers represent the lowest and highest values within the boxes $\pm 1.5x$ the IQR. F) Scattered plot of the first two principal component obtained analysing the dataset. Brackets refers to the amount of variability described by each PC. Asterisk report the results of the student t-test: "*" significant at $p \leq 0.05$; "**" significant at $p \leq 0.01$; "***" significant at $p \leq 0.001$; "n.s" not significant $p > 0.05$.

A similar pattern resulted from a multivariate statistical analysis. By using principal component analysis (PCA) to analyse the data, it appeared clear how the first two PCs distinguished sEVs from PL while IEVs sat in between (Figure 3F) but were more similar to PL. The spectra of the first two PCs are presented in the supplementary information as Figure S4. The spectra of the first two PCs used in the analysis confirmed that most of the variance in the dataset was associated to the peaks relative to carotenoids, aromatic amino-acids and to the protein folding.

Raman characterization of plasma, IEVs and sEVs in SALS patients.

Raman spectra of PL, IEVs and sEVs were collected from a cohort of 20 SALSs and of 20 HCs in order to explore the biochemical differences in EVs and plasma that might be associated to the disease.

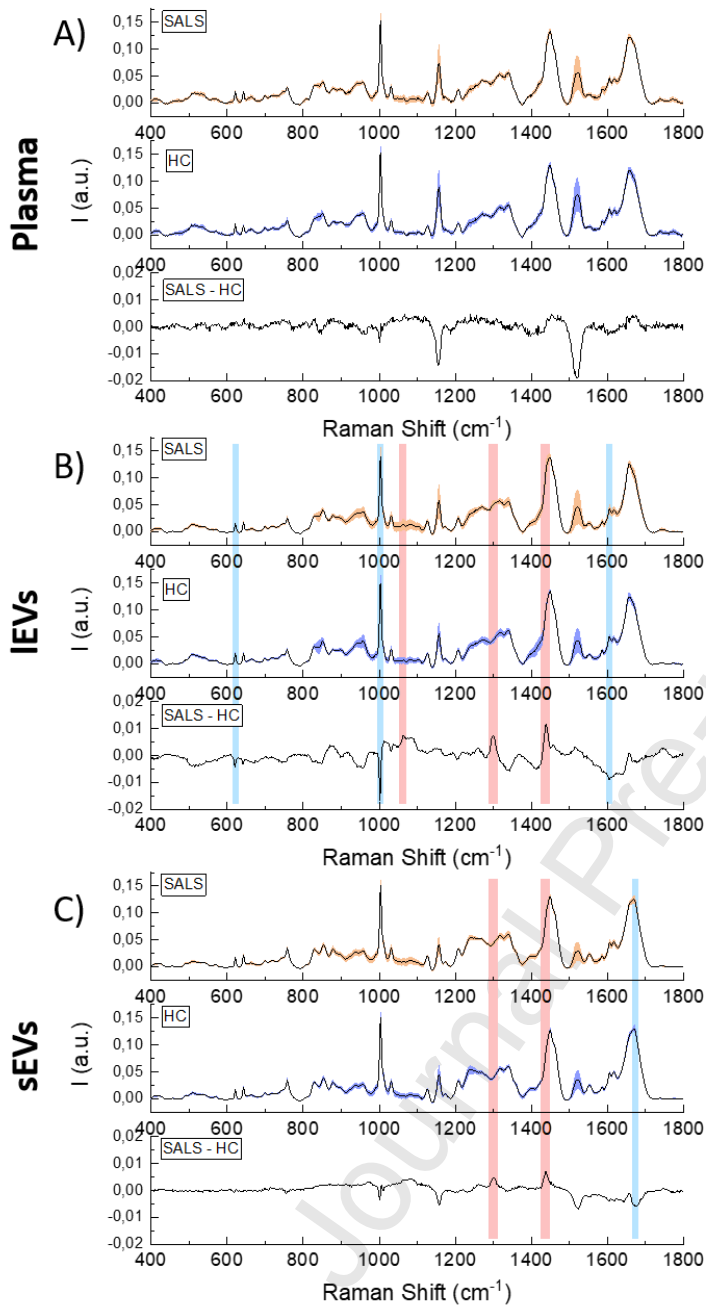


Figure 4. A) Raman spectra of PL in SALS (top) and in the HC subjects (middle). At the bottom it is represented the differential spectra of the two groups B) Raman spectra of IEVs in SALS (top) and in the HC subjects (middle). At the bottom it is represented the differential spectra of the two groups. C) Raman spectra of sEVs in SALS (top) and in the HC subjects (middle). At the bottom it is represented the differential spectra of the two groups. The main line is the average of all subjects included. Shaded areas represent the standard deviation of the intensity. Bands shows statistically

significant different peaks (at least $p < 0.05$). Light blue bands represent peaks that are more intense in the HC group. Pink bands represent peaks that are more intense in SALS patients.

Figure 4 shows the mean spectrum of PL, IEVs and sEVs collected from SALS subjects (top) from the HC groups (middle) and the differential spectra between the two groups for each preparation.

When plasma sample of SALSs and HCs were analysed we observed variations only on the peaks relative to carotenoids at 1156 and 1519 cm^{-1} . However, the difference between the two subjects groups were not statistically significant. The box plot of the difference observed on the carotenoid's peaks in PL of SALSs and HCs are provided in Figure S5.

However, IEVs from SALSs compared to IEVs of HCs were particularly rich in lipids as shown by the highest intensity of the peaks at 1063, 1298, and 1437 cm^{-1} . In particular, the bands at 1437 and at 1298 cm^{-1} that appeared as shoulder in the lipids peaks suggested that, not only the amount of lipids was higher in IEVs of SALSs, but also the biochemical profiles of lipids could be different. Besides, the peaks relative to the aromatic amino acid phenylalanine at 621, 1002 and 1604 cm^{-1} were significantly less intense in SALSs, suggesting that they are characterized by an altered protein content.

The Raman analysis of sEVs (Figure 4C) showed different result from both IEVs and PL confirming the independent nature of the biomaterials. In particular, we observed that sEVs from ALS patients had slightly higher peaks relative to lipids compared to HCs (peaks at 1298 and 1437 cm^{-1} were statistically different from the one observed in the HC) but no differences associated to aromatic aminoacids were detected. On the other hand, sEVs of ALS patients were associated with a lower peak at 1670 cm^{-1} of the Amide I bond.

Figure 5 shows the box plot of the intensities of the peaks with statistically significant ($p < 0.05$) differences between SALSs and HCs.

Overall, our data confirmed the differences observed between SALSs and HCs are different in the three set of data of three different bio-samples.

A further analysis was done to check if differences could emerge between fast and slow SALS patients but no statistical significant differences was found (Figure S6).

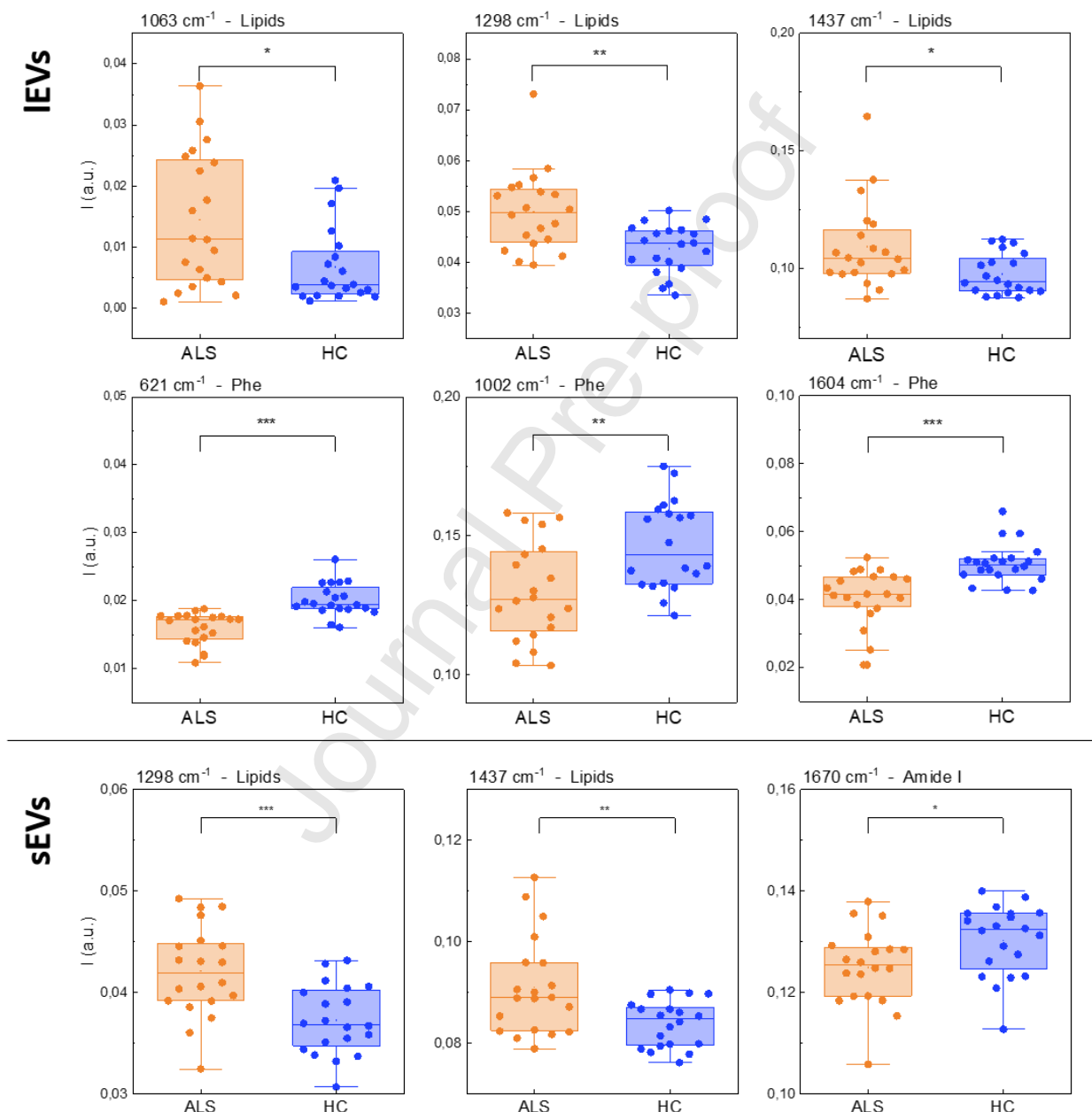


Figure 5: Box plot showing the different intensity of selected peaks of in the spectra of IEVs (top and middle line) and sEVs (bottom line) between SALSs (orange) and HCs (blue). Data are shown

as box and whiskers plots. Each data point represents a single subject acquired. Each box represents the 25th to 75th percentiles (interquartile range [IQR]). Lines inside the boxes represent the median. The whiskers represent the lowest and highest values within the boxes $\pm 1.5x$ the IQR. Asterisk report the results of the student t-test: “*” significant at $p \leq 0.05$; “**” significant at $p \leq 0.01$; “***” significant at $p \leq 0.001$; “n.s.” not significant $p > 0.05$.

Classification of HC and SALS subjects by RS analysis

To understand the potential of RS analysis for the classification of SALS and HC subjects, we also performed a principal component analysis on the dataset obtained from PL, IEVs and sEVs. For each bio-samples we selected the PC more able to distinguish the two groups of subjects and we analysed the results. Table S2 in supplementary information reports the main parameters of the first three PCs calculated for each bio-samples. PC1 relative to PL (61 % of the variability) referred mostly to the carotenoids peaks previously identified as the most prominent difference between the two subjects groups. The score of PC1 however was not statistically significant difference between SALSs and HCs and the AUC of its ROC curve was just of 64,5%.

In the analysis of IEVs, PC3 (11 % of the variability) was the one that could be related to the differences between SALSs and HCs subjects in the dataset. This was confirmed by the fact that the spectrum related with PC3 (Figure 6D) closely matched the difference spectrum between the two subjects groups. The score of PC3 resulted significantly different between the two subjects groups (Figure 6E) and the ROC curve obtained on these values showed an AUC of 84% suggesting the presence of real biochemical differences between SALSs and HCs (Figure 6F).

Even in the analysis performed on sEVs, PC3 (13 % of the variability) referred to the differences observed between SALS and HC subjects. However, given the less pronounced differences

observed, the results of the classification performed on sEVs was less informative and the AUC of the ROC curve is just of 64% (Figure 5I).

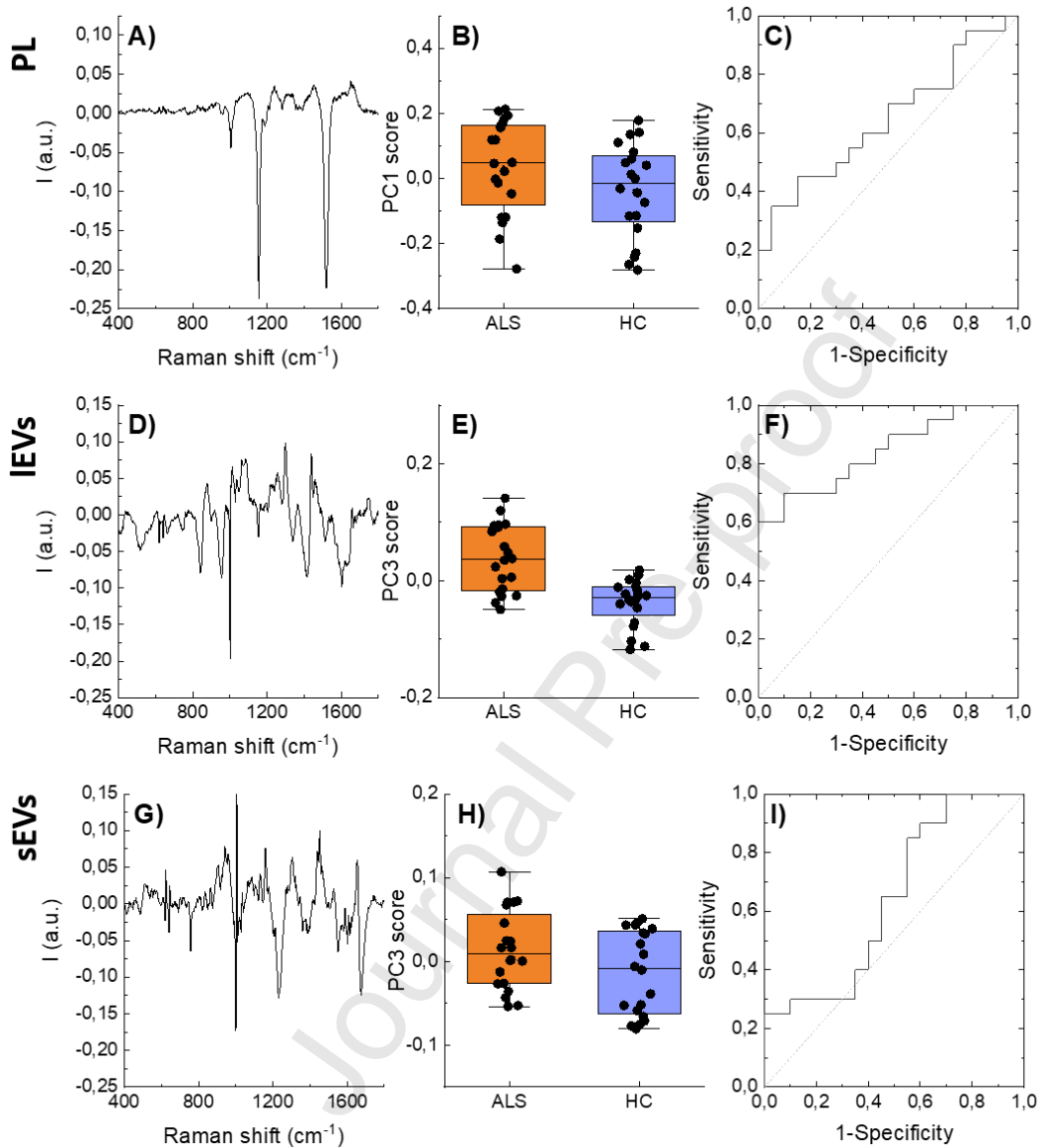


Figure 6: A) Raman spectrum of PC1 from PL of SALS and HC subjects. B) Score of the PC1 obtained by PCA analysis performed on PL. C) ROC curve obtained on the score of PC1 of PL. D) Raman spectrum of PC3 from IEVs of SALS and HC subjects. E) Score of the PC3 obtained by PCA analysis performed on IEVs. F) ROC curve obtained on the score of PC3 of IEVs. G) Raman spectrum of PC3 from sEVs of SALS and HC subjects. H) Score of the PC3 obtained by PCA analysis performed on sEVs. I) ROC curve obtained on the score of PC3 of sEVs. Data are shown

as box and whiskers plots. Each data point represents a single subject included in the study. Each box represents the 25th to 75th percentiles (interquartile range [IQR]). Lines inside the boxes represent the median. The whiskers represent the lowest and highest values within the boxes $\pm 1.5 \times$ the IQR

DISCUSSION:

Amyotrophic Lateral Sclerosis is a fatal neurodegenerative disease that does not have diagnostic and prognostic biomarkers. In this work, we used Raman Spectroscopy to identify possible differences between types of extracellular vesicles and plasma and if any functional group could possibly distinguish sporadic ALS patients from healthy controls. On the first point, we demonstrated how IEVs, sEVs and PL were characterized by clearly different biochemical profiles even if we have described a partial biochemical overlap between IEVs and PL. In particular, plasma had more pronounced peak of carotenoids compared to EVs as they mostly travel within lipoproteins, lost during EVs preparation (30). On the contrary, Amide III and Amide I were overrepresented in EVs, in particular in sEVs compared to IEVs. This data underline that EVs were characterized by an increase of the peaks relative to beta folded proteins at 1239 and 1675 cm^{-1} (26). The band relative to lipids was very similar in PL and IEVs but was much less intense in sEVs. sEVs were also rich in tryptophan compared to IEVs and plasma (25).

The different biochemical profiles of PL, IEVs and sEVs confirmed the different biochemical roles of IEVs and sEVs and thus support the decision to analyse them independently in the case-control study.

The main novelty of this manuscript was that IEVs in plasma of SALS patients have a different biochemical profile from HC subjects. On the contrary, plasma and sEVs resulted to be rather homogeneous between SALSs and HCs.

In fact, IEVs from SALS patients were particularly rich of lipids and had a lower amount of the aromatic amino acid phenylalanine, which could reflect differences in the protein content of IEVs. The differences referred to lipids found on sEVs of ALS patients compared to HCs were much less marked than the one found on IEVs. sEVs of ALS patients were also different from HCs for a slight lower Amide I peak.

Interestingly, the fact that in IEVs many peaks relative to lipids had different intensity while, on the contrary, plasma spectra were homogeneous between cases and controls analysed support the fact that the difference observed are not due to protein contamination but reflect the real biochemical composition of IEVs.

These results highlights the role of lipids in SALSs and are in accordance with other studies on the topic. Blasco et al. showed that ALS patients displayed a highly significant specific lipidomic signature compared to control in cerebrospinal fluid (CSF). Phosphatidylcholine PC (36:4), ceramides and glucosylceramides were the predominant classes in SALS patients compared to HCs (31). One of latest GWAS showed hyperlipidemia as a causal risk factor for ALS (32). This is highly supported by other authors since low IDL-B levels and the high levels of the cholesterol-rich LDL-1 subfraction is consistent with previously reported hypercholesterolemia (33, 34). However, to the best of our knowledge, our work is the first study that gives hints about different lipid signature in extracellular vesicles of SALS patients. We can hypothesis that the brain, the primarily affected organ in ALS, is the richest organ in lipids and motor neuron death might disrupt the lipid organization of the pre-synaptic membrane affecting membrane trafficking (35) and IEVs lipid cargo. In fact, one of the key pathogenic process of ALS is the endolysosomal and autophagic defects and since lysosomes mediate the clearance of lipids, lipid storage might be compromised (36). Moreover, oxysterols, mainly 25-hydroxycholesterol and its metabolites are involved (37) and might trigger the immune response and this can also be in line with our previous finding of enhanced leukocyte derived IEVs (19).

On the other hand, peaks relative to phenylalanine were significantly less intense in IEVs from SALSs. This suggests a possible altered protein content in IEVs from SALSs as we have previously showed (7, 18). Moreover, phenylalanine is also a precursor for tyrosine, the monoamine neurotransmitters dopamine, norepinephrine, and epinephrine (38). It was proven that cultured neurons from embryonic and mature mammalian neural tissue release EVs after stimulation with depolarization or excitation with Ca^{2+} ionophores, GABA receptor blockers, AMPA or NMDA and can transport neurotransmitters (39) in the brain. In ALS it was found a significantly reduced striatal DA transporter expression in patients with bulbar- or limb-onset compared to controls, however, no differences in spinal DA concentrations were found between SALS and control subjects (40). We can hypothesize a decrease of neurotransmitters release by IEVs in plasma of ALS patients, but these data need to be confirmed.

In our preliminary data we also divided patients according to the progression rate of the disease in slow and fast progressing patients as previously described in the literature (17). No statistically difference was detected between these two groups, however it would be important to confirm these data on a bigger cohort of patients. It is also true that SALS patients requires a better stratification than progression rate for the development of a therapeutic approach. This was confirmed by a recent study which proposed a new approach for machine learning and clustering ALS patients using data from >10,000 patients from ALS clinical trials and patients from community-based patient registers (41).

Overall, our results demonstrated that IEVs are a promising biomarker for the diagnosis of ALS. Besides, from the biomedical point of view, our study also supports the involvement of lipids and phenylalanine metabolism in IEVs of SALS patients paving the road for other studies on this topic. Future study will be necessary to understand better the relationship between the observed variation in the biochemical profile of IEVs and the pathologic processes involved in SLA. In particular, the

study of IEVs specifically released by neuronal cells might provide more detailed information and a better classification of ALS patients.

Author Contributions

The manuscript was written through contributions of all authors. All authors have given approval to the final version of the manuscript.

Both authors contributed equally to this manuscript

Notes

Conflict of interest: nothing to declare.

ACKNOWLEDGMENT:

Project was partially funded by the project 5xmille 2017 Enti di ricerca sanitaria Fondazione Maugeri, by Fondazione Regionale Ricerca Biomedica (TRANS-ALS)-(2015-0023), and by Italian Ministry of Health (GR-2016-02361552).

REFERENCES:

- 1 Brown RH, Al-Chalabi A. Amyotrophic Lateral Sclerosis. *N. Engl. J. Med.* 2017; 377(2): 162-172.
- 2 Verber NS, Shephard SR, Sassani M et al. Biomarkers in Motor Neuron Disease: A State of the Art Review. *Front Neurol.* 2019(3);10:291.

- 3 Goetzl EJ, Mustapic M, Kapogiannis D, et al. Cargo proteins of plasma astrocyte-derived exosomes in Alzheimer's disease. *FASEB J.* 2016; **30**: 3853-3859.
- 4 Raposo G, Stoorvogel W. Extracellular vesicles: exosomes, microvesicles, and friends. *J. Cell Biology.* 2013; **200**: 373–383.
- 5 György B, Szabó TG, Pásztói M, et al. Membrane vesicles, current state-of-the-art: emerging role of extracellular vesicles. *Cellular and Molecular Life Sciences.* 2011; **68**: 2667-2688.
- 6 Théry C, Witwer KW, Aikawa E, et al. Minimal information for studies of extracellular vesicles 2018 (MISEV2018): a position statement of the International Society for Extracellular Vesicles and update of the MISEV2014 guidelines *J. Extracellular Vesicles.* 2018; **7**: 1535750.
- 7 Sproviero D, La Salvia S, Giannini M, et al. Pathological Proteins Are Transported by Extracellular Vesicles of Sporadic Amyotrophic Lateral Sclerosis Patients. *Front. Neurosci.* 2018; **12**: 487.
- 8 Revenfeld AL, Bæk R, Nielsen MH, et al. Diagnostic and Prognostic Potential of Extracellular Vesicles in Peripheral Blood. *Clin Ther.* 2014; **36**(6): 830-46.
- 9 Butler HJ, Ashton L, Bird B, et al. Using Raman spectroscopy to characterize biological materials *Nature Protocols.* 2016; **11**: 664–687.
- 10 Byrne HJ, Knief P, Keating ME, Bonnier F. Spectral pre and post processing for infrared and Raman spectroscopy of biological tissues and cells. *Chem. Soc. Rev.* 2016; **45**: 1865-1878.
- 11 Krafft C, Wilhelm K, Eremin A, et al. A specific spectral signature of serum and plasma-derived extracellular vesicles for cancer screening. *Nanomedicine: Nanotechnology, Biology and Medicine.* 2017; **13**: 835-841.
- 12 Lee W, Nanou A, Rikkert L, et al. Label-Free Prostate Cancer Detection by Characterization of Extracellular Vesicles Using Raman Spectroscopy. *Anal Chem.* 2018; **90**: 11290-11296.

- 13 Gualerzi A, Niada S, Giannasi C, et al. Raman spectroscopy uncovers biochemical tissue-related features of extracellular vesicles from mesenchymal stromal cells. *Scientific Report*. 2017; **77**: 9820.
- 14 Kruglik SG, Royo F, Guigner J-M, et al. Raman tweezers microspectroscopy of circa 100 nm extracellular vesicles. *Nanoscale*, 2019; **11**: 1661-1679.
- 15 Gualerzi A, Picciolini S, Carlomagno C, et al. Raman profiling of circulating extracellular vesicles for the stratification of Parkinson's patients. *Nanomedicine*. 2019; **22**: 102097.
- 16 Brooks BR., Miller RG, Swash M, et al. El Escorial revisited: revised criteria for the diagnosis of amyotrophic lateral sclerosis. *Amyotroph. Lateral. Scler. Other Motor Neuron. Disord*. 2000; 1(5), 293-299.
- 17 Lu CH, Macdonald-Wallis C, Gray E et al. Neurofilament light chain: a prognostic biomarker in amyotrophic lateral sclerosis. *Neurology*. 2015; **84**: 2247–2257.
- 18 They, C., Amigorena, S., Raposo, G., Clayton, A. Isolation and characterization of exosomes from cell culture supernatants and biological fluids. *Curr. Protoc. Cell. Biol*. 2006, 3(22), 3.22.1-3.22.29.
- 19 Sproviero D, La Salvia S, Colombo F et al. Leukocyte Derived Microvesicles as Disease Progression Biomarkers in Slow Progressing Amyotrophic Lateral Sclerosis Patients. *Front Neurosci*. **2019**; 13:344.
- 20 Eilers PHC, Boelens HFM. Baseline correction with asymmetric least squares smoothing 2005, Leiden University Medical Centre report. https://zanran_storage.s3.amazonaws.com/www.science.uva.nl/ContentPages/443199618.pdf (accessed 7th October 2019)
- 21 Rygula A, Majzner K, Marzec KM, et al. J. Raman spectroscopy of proteins: a review. *J Raman Spectr*. 2013; **44**(8): 1061-1076

- 22 Stone N, Kendall C, Smith J, et al. Raman spectroscopy for identification of epithelial cancers. *Faraday Discuss.* 2004; **126**: 141-157.
- 23 De Gelder J, De Gussem K, Vandenabeele P, et al. Reference database of Raman spectra of biological molecules. *J. Raman Spectrosc.* 2007; **38**: 1133–1147.
- 24 Krafft C, Neudert L, Simat T. et al. Near infrared Raman spectra of human brain lipids. *Spectrochim. Acta A Mol. Biomol. Spectrosc.* 2005; **61**(7): 1529-35.
- 25 Talari ACS, Movasaghi Z, Rehman S, et al. Raman spectroscopy of biological tissues. *Appl. Spectr. Rev.* 2015; **50**: 46–111.
- 26 Mahadevan-Jansen A, Richards-Kortum RR. Raman spectroscopy for the detection of cancers and precancers. *J. Biomed. Opt.* 1996; **1**(1): 31-70.
- 27 Vanna R, Ronchi P, Lenferink ATM, et al. Label-free imaging and identification of typical cells of acute myeloid leukaemia and myelodysplastic syndrome by Raman microspectroscopy *Analyst.* 2015; **140**: 1054–1064.
- 28 Faoláin EO, Hunter MB, Byrne JM, et al. A study examining the effects of tissue processing on human tissue sections using vibrational spectroscopy *Vibr. Spectr.* 2005; **38**: 121-127.
- 29 Casella M, Lucotti A, Tommasini M, et al. Raman and SERS recognition of Beta-Carotene and Haemoglobin fingerprints in Human Whole Blood. *Spectrochim. Acta. A. Mol. Biomol. Spectrosc.* 2011; **79**(5): 915-919.
- 30 Bjornson LK, Kayden HJ, Miller E, et al. The transport of α -tocopherol and β -carotene in human blood *J. Lipid Res.* 1976; **17**: 343-352.
- 31 Blasco H, Veyrat-Durebex C, Bocca C et al. Lipidomics Reveals Cerebrospinal-Fluid Signatures of ALS. *Sci Rep.* 2017; **7**(1):17652.
- 32 Bandres-Ciga S, Noyce AJ, Hemani G et al. Shared polygenic risk and causal inferences in amyotrophic lateral sclerosis. *Ann Neurol.* 2019; **85**:470-481.

- 33 Delaye JB, Patin F, Piver E et al. Low IDL-B and high LDL-1 subfraction levels in serum of ALS patients. *J Neurol Sci.* 2017; **15**(380):124-127.
- 34 Rafiq MK, Lee E, Bradburn M et al. Effect of lipid profile on prognosis in the patients with amyotrophic lateral sclerosis: Insights from the olesoxime clinical trial. *Amyotroph Lateral Scler Frontotemporal Degener.* 2015; **16**(7-8): 478-84.
- 35 Tracey TJ, Steyn FJ, Wolvetang EJ, Ngo ST. Neuronal Lipid Metabolism: Multiple Pathways Driving Functional Outcomes in Health and Disease. *Front Mol Neurosci.* 2018; **23**:11:10.
- 36 Miranda AM and Di Paolo G. Endolysosomal dysfunction and exosome secretion: implications for neurodegenerative disorders. *Cell Stress.* 2018; **2**(5): 115-118.
- 37 Sung-Min K, Min-Young N, Heejaung K et al. 25-Hydroxycholesterol is involved in the pathogenesis of amyotrophic lateral sclerosis. *Oncotarget.* 2017; **8**(7): 11855–11867.
- 38 Fernstrom JD, Fernstrom MH. Tyrosine, phenylalanine, and catecholamine synthesis and function in the brain. *J Nutr.* 2007;**137**(6 Suppl 1):1539S-1547S; discussion 1548S.
- 39 Borasio GD, Linke R, Schwarz J et al. Dopaminergic deficit in amyotrophic lateral sclerosis assessed with [I-123] IPT single photon emission computed tomography. *J. Neurol. Neurosurg. Psychiatry.* 1998; **65**, 263–265.
- 40 Bertel O., Malessa S., Sluga E., Hornykiewicz O. Amyotrophic lateral sclerosis: changes of noradrenergic and serotonergic transmitter systems in the spinal cord. *Brain Res.* 1991; **566**, 54–60.
- 41 Kueffner R, Zach N, Bronfeld M et al. Stratification of amyotrophic lateral sclerosis patients: a crowdsourcing approach. *Sci Rep.* 2019; **9**(1):690.

Graphical Abstract:

Plasma, large extracellular vesicles (IEVs) and small extracellular vesicles (sEVs) from patients affected by Amyotrophic Lateral Sclerosis (ALS) and from a cohort of matched healthy controls were studied by means of Raman spectroscopy. The results obtained show that Raman spectroscopy is able to identify a specific fingerprint of each specimen and that the IEVs of ALS patients are characterized by a distinct biochemical composition. This study thus paves the road towards the use of IEVs as possible circulating biomarkers of ALS.

Journal Pre-proof